

Simulating star-forming regions in spiral galaxies with AMUSE

Steven Rieder^{1,2} , Clare Dobbs¹ and Thomas Bending¹

¹School of Physics and Astronomy, University of Exeter, Stocker Road,
Exeter EX4 4QL, United Kingdom

²RIKEN Center for Computational Science, 7-1-26 Minatojima-minami-machi,
Chuo-ku, Kobe, 650-0047, Hyogo, Japan

Abstract. We present a model for hydrodynamic + N-body simulations of star cluster formation and evolution using **AMUSE**. Our model includes gas dynamics, star formation in regions of dense gas, stellar evolution and a galactic tidal spiral potential, thus incorporating most of the processes that play a role in the evolution of star clusters.

We test our model on initial conditions of two colliding molecular clouds as well as a section of a spiral arm from a previous galaxy simulation.

Keywords. galaxies: star clusters; galaxies: spiral; methods: n-body simulations

1. Introduction

Spiral arms are the birth places of star clusters in disc galaxies. The strength of these may affect how the stars are distributed over time.

Where previous work on this topic has focused on either isolated clusters or the large scale structure, we intend to create a model that includes all of the most relevant physics. We use this model to study the formation and longevity of groups of stars in a galactic environment.

2. Method

The simulations in this project involve distance scales ranging from a few hundred parsec to several hundreds of au, while the physics involved includes gravity, hydrodynamics and stellar evolution. Since most simulation programmes are designed to work on only one specific scale and usually are not designed to handle multiple physical processes, we employ **AMUSE**† (Portegies Zwart *et al.* 2009; Pelupessy *et al.* 2013; Portegies Zwart & McMillan 2018) for our simulations. We combine a state-of-the-art SPH code with a direct N-body code, a stellar evolution code, and a galactic tidal field, creating a self-consistent simulation method that follows the early evolution of stellar regions. We resolve stellar masses down to $0.08 M_{\odot}$.

3. Simulation model

We base our model on the simulation method used in Sills *et al.* (2018), which we expand to include more realistic treatment of gas, star formation, and a background potential for the galaxy. Each of these components can be run separately or in combination with the other components, to create the desired simulation environment (Rieder 2019).

† Astrophysical Multipurpose Software Environment

3.1. Gas component

For the gas dynamics, we use the modern SPH code **Phantom** (Price *et al.* 2018), which we integrate in **AMUSE**. **Phantom** natively supports the gas and sink particles needed for our method, and is parallelised using OpenMP and MPI. We let **AMUSE** handle the creation of sinks, by stopping the code when a gas particle reaches a critical density. We then create a sink particle which absorbs gas within a specified radius. This particle is then added to **Phantom**, which handles further accretion of gas onto the sinks.

Since the mass resolution of gas in our simulation is $\sim 1M_{\odot}$, sinks do not represent individual stars, but rather collapsing parts of the cloud. We let sinks form stars, sampled from a Kroupa (2001) IMF, until not enough mass remains to form the next mass from the sample (similar to Wall *et al.* 2019). To make sure we have a well-sampled IMF, we set the parameters for sink creation such that each sink will have 150 to $200M_{\odot}$ at the time of formation.

3.2. Stellar component

Stars are dynamically integrated with a direct N-body code. Here, we use the **Hermite** (Hut *et al.* 1995) integrator. However, since we expect several groups of stars to form which will have little interaction with each other, we plan to use an approach that combines a direct N-body method with a tree method (such as in Iwasawa *et al.* 2017).

We combine this with the **SeBa** (Portegies Zwart & Verbunt 1996; Toonen *et al.* 2012) stellar evolution code, which sets the maximum allowed timestep for stellar dynamics to a fraction of the stellar evolution timescale. We use **SeBa** to primarily update the stellar masses, though it also informs us of the current phase in the stars' lifetimes.

3.3. Coupling with a tidal field

We use the **Bridge** module in **AMUSE** (based on Fujii *et al.* 2007) to couple the gravitational dynamics from gas and sinks in the gas component with the stellar component. **Bridge** also supports coupling these with other external potentials, such as a (time-dependent) tidal field. These potentials may be analytic, but they can also be in the form of tidal tensors (e.g. Rieder *et al.* 2013).

4. Tests

We test our model with both a colliding clouds test and using a spiral arm section of a galaxy simulation.

4.1. Colliding clouds

We generate initial conditions consisting of a turbulent molecular gas cloud ($150,000 M_{\odot}$, $80 \times 28 \times 28$ parsec) which is duplicated and shifted along the x-axis. The two resulting clouds then receive a relative velocity of 48 km/s. In Figure 1 we show snapshots of this simulation at 0.5, 1.0 and 1.5 Myr. Since our model currently does not have a source of feedback to prevent star formation, a too large fraction of the gas will be converted into stars.

4.2. Spiral arm test

As initial conditions we take a $500 \times 500 \times 500$ parsec region from Dobbs & Pringle (2013), which we re-sample to a resolution of $1M_{\odot}$ per particle (Bending *et al.* submitted). For this simulation we include the same tidal field as in the original galaxy simulation (Dobbs & Pringle 2013), which consists of a logarithmic disk potential for the galactic

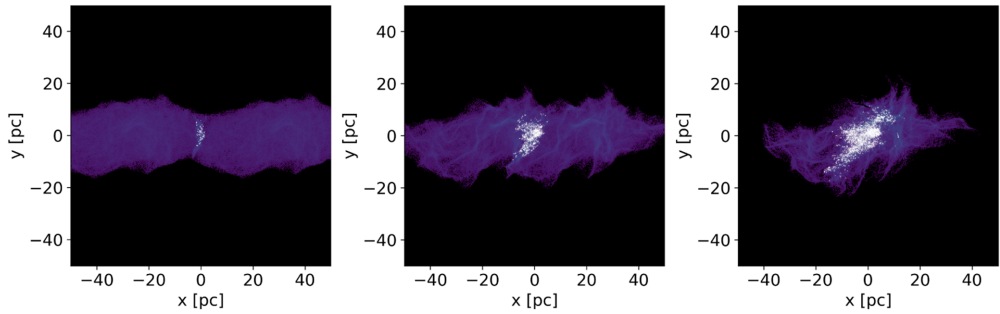


Figure 1. Colliding clouds simulation at 0.5, 1.0 and 1.5 Myr. White dots represent stars, while red dots represent sink particles.

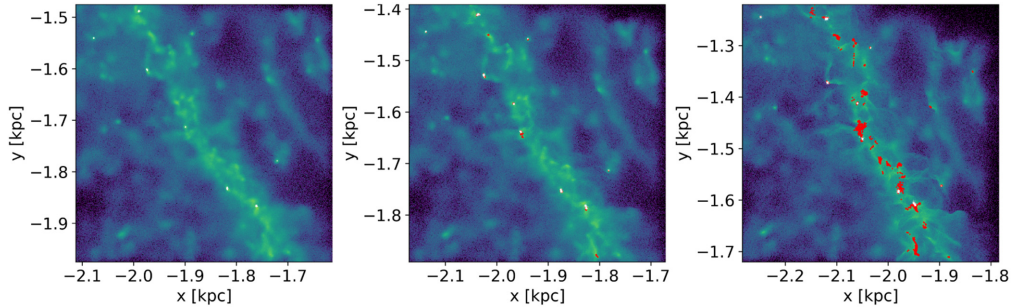


Figure 2. Spiral arm simulation at 0.5, 1.0 and 2.0 Myr, as in Figure 1. In this simulation, we stop the formation of individual stars after 0.8 Myr, while sink particles still continue to form.

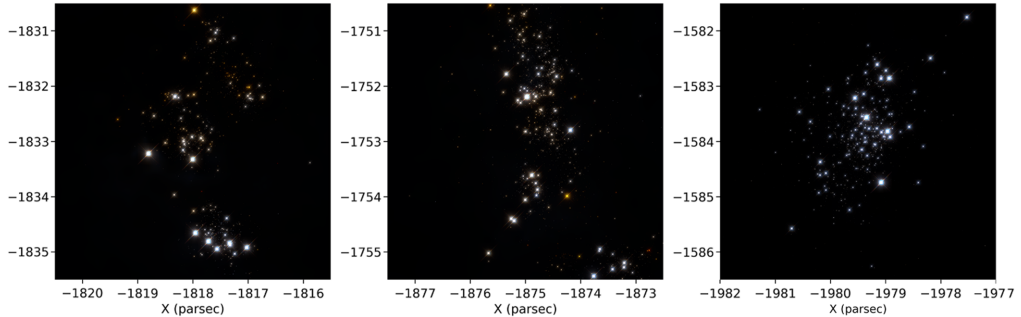


Figure 3. Zoom in on one of the star forming regions of Figure 2, at 0.5, 1.0 and 2.0 Myr. Visualisation is done with Fresco (Rieder & Pelupessy 2019), and includes extinction by dust using a fixed gas-to-dust ratio.

disk (Binney & Tremaine 2008) and an additional component for the spiral arms (Cox & Gómez 2002).

After 0.8 Myr, we turn off the formation of stars from sinks, both to trace only the evolution of the first batch of stars and to prevent the N^2 -scaling stellar gravity calculations from dominating the simulation runtime.

In Figure 2 we show snapshots of this simulation at 0.5, 1.0 and 2.0 Myr. Star formation happens predominantly in the spiral arm. In Figure 3, we zoom in on one of the star forming regions. During this time, the cluster starts to collapse from individual cores to a more spherical star cluster.

5. Conclusions

We present a model for simulating star-forming regions in a self-consistent manner, including gas dynamics, the formation of stars, stellar evolution and a large-scale environment. While our model succeeds in simulating such regions, we currently lack a source of feedback to prevent overly dense regions and too much star formation from occurring.

References

- T. J. R. Bending, C. L. Dobbs & M. R. Bate (submitted to *MNRAS*, 2019)
- J. Binney & S. Tremaine 2008
- D. P. Cox & G. C. Gómez. *ApJS*, 142(2):261–267, Oct 2002
- C. L. Dobbs & J. E. Pringle. *MNRAS*, 432(1):653–667, Jun 2013
- M. Fujii, M. Iwasawa, Y. Funato, & J. Makino. *PASJ*, 59:1095, Dec 2007
- P. Hut, J. Makino, & S. McMillan. *ApJ*, 443:L93, Apr 1995
- M. Iwasawa, S. Oshino, M. S. Fujii, & Y. Hori. *PASJ*, 69(5):81, Oct 2017
- P. Kroupa. *MNRAS*, 322(2):231–246, Apr 2001
- F. I. Pelupessy, A. van Elteren, N. de Vries, S. L. W. McMillan, N. Drost, & S. F. Portegies Zwart. *A&A*, 557:A84, Sep 2013
- S. Portegies Zwart and S. McMillan. 2514-3433. IOP Publishing, 2018. ISBN 978-0-7503-1320-9. URL <http://dx.doi.org/10.1088/978-0-7503-1320-9>
- S. Portegies Zwart, S. McMillan, S. Harfst, D. Groen, M. Fujii, B. Ó. Nualláin, E. Glebbeek, D. Heggie, J. Lombardi, P. Hut, V. Angelou, S. Banerjee, H. Belkus, T. Fragos, J. Fregeau, E. Gaburov, R. Izzard, M. Jurić, S. Justham, A. Sotoriva, P. Teuben, J. van Bever, O. Yaron, & M. Zemp. *New Astron.*, 14(4):369–378, May 2009
- S. F. Portegies Zwart & F. Verbunt. *A&A*, 309:179–196, May 1996
- D. J. Price, J. Wurster, T. S. Tricco, C. Nixon, S. Toupin, A. Pettitt, C. Chan, D. Mentiplay, G. Laibe, S. Glover, C. Dobbs, R. Nealon, D. Liptai, H. Worpel, C. Bonnerot, G. Dipierro, G. Ballabio, E. Ragusa, C. Federrath, R. Iaconi, T. Reichardt, D. Forgan, M. Hutchison, T. Constantino, B. Ayliffe, K. Hirsh, & G. Lodato. *Publ. Astron. Soc. Australia*, 35:e031, Sep 2018
- S. Rieder, July 2019. URL <https://doi.org/10.5281/zenodo.3356923>
- S. Rieder & F. I. Pelupessy, July 2019. URL <https://doi.org/10.5281/zenodo.3355548>
- S. Rieder, T. Ishiyama, P. Langelaan, J. Makino, S. L. W. McMillan, & S. Portegies Zwart. *MNRAS*, 436(4):3695–3706, Dec 2013
- A. Sills, S. Rieder, J. Scora, J. McCloskey, & S. Jaffa. *MNRAS*, 477(2):1903–1912, Jun 2018
- S. Toonen, G. Nelemans, & S. Portegies Zwart. *A&A*, 546:A70, Oct 2012
- J. E. Wall, S. L. W. McMillan, M.-M. Mac Low, R. S. Klessen, & S. Portegies Zwart. *arXiv e-prints*, art. [arXiv:1901.01132](https://arxiv.org/abs/1901.01132), Jan 2019